

# Guardian: Detecting Robotic Planning and Execution Errors with Vision-Language Models

Paul Pacaud\*, Ricardo Garcia\*, Shizhe Chen\*, Cordelia Schmid\*

**Abstract**— Robust robotic manipulation requires reliable failure detection and recovery. Although current Vision-Language Models (VLMs) show promise, their accuracy and generalization are limited by the scarcity of failure data. To address this data gap, we propose an automatic robot failure synthesis approach that procedurally perturbs successful trajectories to generate diverse planning and execution failures. This method produces not only binary classification labels but also fine-grained failure categories and step-by-step reasoning traces in both simulation and the real world. With it, we construct three new failure detection benchmarks: **RLBench-Fail**, **BridgeDataV2-Fail**, and **UR5-Fail**, substantially expanding the diversity and scale of existing failure datasets. We then train **Guardian**, a VLM with multi-view images for detailed failure reasoning and detection. **Guardian** achieves state-of-the-art performance on both existing and newly introduced benchmarks. It also effectively improves task success rates when integrated into a state-of-the-art manipulation system in simulation and real robots, demonstrating the impact of our generated failure data.

## I. INTRODUCTION

Despite recent advances in task planning and action execution enabled by Large Language Models (LLMs) [1], [2] and Vision-Language Models (VLMs) [3], current robotic manipulation systems remain vulnerable to a wide range of failures [4], [5], [6]. They can suffer from incorrect task plans [7] due to LLM hallucinations [8], perception errors such as confusing similar objects [9], [10], and low-level control issues such as unstable grasps or slippage [11]. These failures often compound during task execution, severely hindering the reliability of robots in real-world scenarios. To improve robustness, there is a growing interest in models that can leverage vision and language to reason about task execution and detect robot failures [12], [13], [14].

A key challenge in robotic failure detection is the lack of comprehensive failure datasets. Most real-world robot datasets consist of successful demonstrations [15], [16], [17], offering limited insight into failure modes. Automatically collecting failures by running trained policies is slow and unsafe, while manually collecting failure data [13], [18] is labor-intensive and often lacks diversity and realism. As a result, prior work [14] largely relies on simulation to construct failure cases, which however suffers from the notorious sim-to-real gap [19]. Furthermore, they predominantly focus on execution errors, with limited coverage of planning failures [14] and lack fine-grained failure reasons [12], [20], [14], [13], [18].

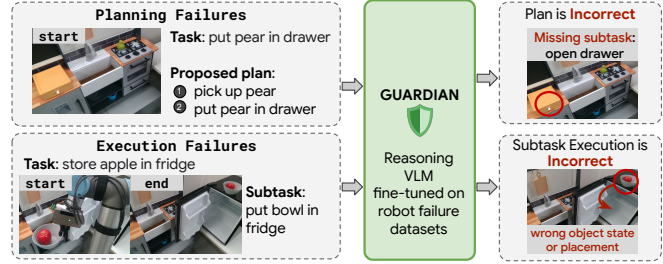


Fig. 1: Illustration of our **Guardian** model - a VLM fine-tuned on our constructed failure datasets. It detects planning failures (top) and execution failures (bottom) in robotic manipulation.

This scarcity of diverse, realistic, and richly annotated failure data significantly hampers the development and evaluation of failure detection methods.

Another challenge is effectively leveraging and reasoning over visual context for failure detection. REFLECT [12] converts images into textual descriptions and then leverages LLM reasoning to detect failures, but this multi-stage pipeline is vulnerable to error accumulation from incomplete or inaccurate image captions. Other recent approaches [20], [21] use VLMs to process images directly, yet typically rely on single-view observations, making them susceptible to occlusions and incomplete scene understanding. AHA [14] addresses this by concatenating multi-view images across timesteps into a single grid-based representation; although this expands visual coverage, the compressed format can hinder fine-grained spatial-temporal understanding. Moreover, most existing methods output categorical labels without providing explicit reasoning traces, limiting interpretability and the ability to diagnose complex failure modes.

To address these challenges, we introduce an automatic failure generation approach that produces diverse planning and execution failures, and we train a reasoning VLM *Guardian* on the resulting data for robust failure detection. Our method procedurally perturbs successful robot trajectories in both simulation and real-world settings to generate failures annotated with fine-grained categories and step-by-step reasoning traces. Using this pipeline, we construct three new datasets: **RLBench-Fail** (14K execution and 7K planning samples in the RLBench simulator [22]), **BridgeDataV2-Fail** (10K execution and 6K planning samples using the real-robot BridgeDataV2 data [23]), and **UR5-Fail** (570 execution and 370 planning samples), our collected real-robot failure dataset with policy-driven rollouts. We then develop *Guardian*, a reasoning VLM fine-tuned for failure detection. As illustrated in Fig. 1, *Guardian* formulates failure detection as a visual

\* Inria, École normale supérieure, CNRS, PSL Research University [firstname.lastname@inria.fr](mailto:firstname.lastname@inria.fr).

This work has been submitted to the IEEE for possible publication. Copyright may be transferred without notice, after which this version may no longer be accessible.

question-answering task, reasoning over task instructions, subtask descriptions, and the visual scene. It leverages high-resolution, multi-view images to provide fine-grained and interpretable failure categorization. *Guardian* achieves state-of-the-art performance on both *RLBench-Fail* and *BridgeDataV2-Fail*, and generalizes in a zero-shot manner to *RoboFail* [12] and our *UR5-Fail* dataset. We further demonstrate *Guardian*’s plug-and-play capability as a feedback module by integrating it into a robotic manipulation system 3D-LOTUS++ [9]. *Guardian* significantly improves task success through planning and execution monitoring in both simulated and real-world tasks.

In summary, our contributions are three-fold:

- We propose a novel robot failure generation approach that perturbs successful robot demonstrations in both simulation and real-world settings, and autonomously annotates failures with fine-grained categories and reasoning traces. This yields three new datasets for robot failure detection: *RLBench-Fail*, *BridgeDataV2-Fail*, and *UR5-Fail*.
- We introduce *Guardian*, a fine-tuned VLM for planning and execution failure detection. *Guardian* integrates high-resolution, multi-view visual inputs with explicit reasoning to predict fine-grained categorization.
- *Guardian* achieves state-of-the-art performance across four benchmarks, covering both in- and out-of-domain datasets. It further improves task completion of a vision-language manipulation framework in simulated and real robot tasks. We will release datasets, code, and models.

## II. RELATED WORK

**Robot failure datasets.** Existing robot failure datasets cover only limited settings. *RoboFail* [12] provides a small collection of hand-crafted simulation and real-world failures. *Sentinel* [20] generates failures by rolling out a trained policy on out-of-distribution scenarios created through randomizing object scales and poses, but it includes only four tasks. *AHA* [14] perturbs trajectories in *RLBench* simulator [22] to create over 49K image–query pairs, yet the data is restricted to simulation and does not include high-level planning failures. Moreover, none of these datasets provides step-by-step reasoning annotations, limiting the development of models capable of fine-grained failure reasoning. In this work, we propose an automated approach that generates large-scale datasets with diverse planning and execution failures, enriched with fine-grained categories and reasoning traces in both simulation and real-robot environments.

**Failure detection in robotic manipulation.** Traditional monitoring methods rely on explicit models of tasks, identifying model deviations [24], [25]. Unlike LLM-based approaches, they depend on rigid model-based predictions. Recent works formulate failure detection as a Question Answering (QA) task, by zero-shot prompting LLMs and VLMs [20], [21], [13], [26], [27], [28], [29]. For instance, *REFLECT* [12] summarizes multi-sensory inputs as texts, including audio, and feeds the text to an LLM, but its reliance on consecutive off-the-shelf models leads to accumulated errors. Consequently, efforts have been made to fine-tune VLMs

specifically for robotic failure detection. *SuccessVQA* [30] fine-tunes *Flamingo* [31] using both simulated and real-world data, but evaluates only the final task success, while *Guardian* is designed for more granular monitoring, checking the execution of each subtask. Closest to our work, *AHA* [14] fine-tunes *LLaVA-1.5* [32] on multi-class failures generated in *RLBench*. *AHA* concatenates multiple camera viewpoints and keysteps into a single image, leading to compressed visual inputs. Unlike *AHA* and *SuccessVQA*, which treat failure detection as direct classification, *Sentinel* [20] and *Cosmos-Reason1* [33] frame it as a reason-first process with explicit chain-of-thought (CoT) [34] reasoning but focus only on single-view binary failure detection. *Sentinel* proposes a zero-shot CoT prompting framework to leverage off-the-shelf VLMs, while *Cosmos-Reason1* is fine-tuned for physical reasoning. Extending prior approaches, *Guardian* unifies planning and execution verification via chain-of-thought reasoning over separated multi-view inputs, for multi-class failure detection.

**Learning-based robotic manipulation policies.** Recent robotic policies have achieved remarkable performance on manipulation tasks [9], [16], [35], [36]. However, their real-world applicability is still limited by planning and execution errors leading to task failures [11]. Inspired by *Manipulate-Anything* [37] and *Robot Utility Models* [21], which demonstrated significant benefits from integrating VLM verifiers into their pipelines, *Guardian* is designed as a plug-and-play verification module trained on specific failure data. It can seamlessly integrate into existing policies, enhancing robustness by verifying planning and execution stages.

## III. ROBOT FAILURE DATASETS CONSTRUCTION

### A. Data Sources

Simulated data enables controlled failure generation through procedural perturbations [14], while real robot data reduces the sim-to-real gap but requires substantial human supervision [12]. To balance precise control and real-world fidelity, we use both simulated and real-robot datasets to construct robot failure datasets. We propose an automated method that derives planning and execution failures directly from successful demonstrations, avoiding manual failure collection. In both domains, tasks are decomposed into subtasks with corresponding video segments, which form the basis for generating failures. Fig. 2 (middle) illustrates successful episodes from the simulated and real robot datasets.

**Simulated Data.** We use the *RLBench* [22] simulator, selecting 52 tasks from *RLBench-18Task* [38] and *Gem-Bench* [9] benchmarks in our training data. For each task, we generate successful scripted trajectories with varied object placements and segment them into subtasks following 3D-LOTUS++ [9].

**Real Robot Data.** We use *BridgeDataV2* [23] with ECoT annotations [39], which provide fine-grained subtasks and object labels using large VLMs. We further clean these annotations automatically using heuristics and *Mistral-Small-3.1-24B* [1] to filter episodes with missing targets or unreliable

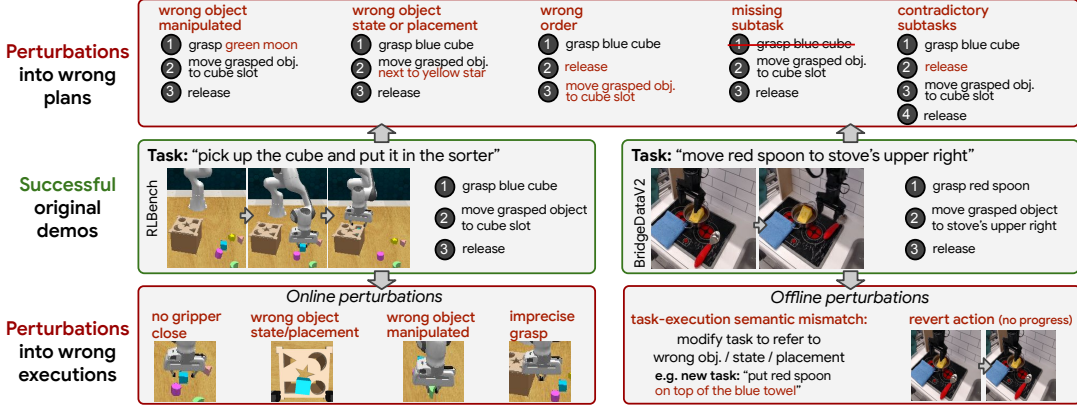


Fig. 2: Failure Data Generation Pipeline. We introduce a novel generation pipeline generating failure cases both online in simulation (RLBench), and offline on the real-world dataset (BridgeDataV2). For each positive example, given its correct plan and successful trajectory, we generate a corresponding incorrect plan and unsuccessful trajectory.

bounding boxes. To increase the number of successful trajectories, we augment data by reversing successful executions when applicable, by swapping their start and end images, and updating the associated instructions accordingly (e.g., “open drawer” becomes “close drawer”, “flip pot upright” becomes “flip pot upside down”). This yields approximately 20% additional successful demonstrations.

### B. Automated Failure Data Generation

We design failure modes based on established failure taxonomies [12], [14] and analysis of robot policy failures [11]. The failures are categorized into two types: planning and execution. A planning error denotes an incorrect decomposition of a task into subplans, whereas an execution error reflects unsuccessful completion of a subplan.

**Planning Failures.** As shown in Fig. 2 (top), we construct five types of planning failures:

- (1) *Wrong object manipulated* – some subtasks manipulate the wrong object.
- (2) *Wrong object state or placement* – some subtasks select the wrong target location, or state for the correct object.
- (3) *Wrong order* – one or several subtasks are not in the correct order, violating causal dependencies.
- (4) *Missing subtask* – required subtasks are missing from the plan, breaking task completeness.
- (5) *Contradictory subtasks* – some subtasks conflict with each other.

Types 1-3 are generated using an LLM (Mistral-Small-24B) to subtly alter the plan, while types 4-5 are created through rule-based perturbations. Each planning example comprises the task instruction, plan, and the initial front-view image.

**Execution Failures.** In simulation, we directly perturb subtask-level actions (Fig. 2, bottom left), leveraging the simulator’s precise control. A randomly selected subtask on the trajectory is modified using four failure modes:

- (1) *No gripper close* – the gripper is correctly positioned to grasp the object, but it fails to close its jaws.
- (2) *Wrong object state or placement* – the correct object is manipulated but ends in an incorrect state or placement.
- (3) *Wrong object manipulated* – the wrong object is used.

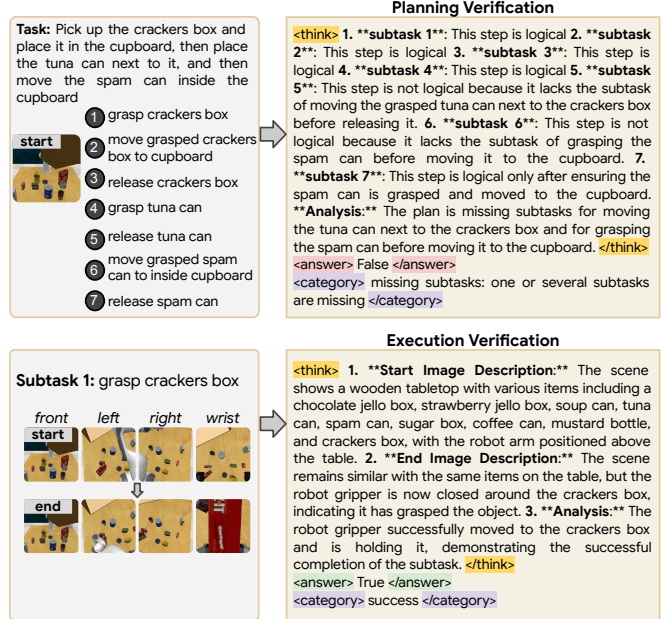


Fig. 3: Training examples. Guardian is trained on reasoning traces produced by our automatic data generation pipeline.

- (4) *Imprecise grasping/pushing* – the gripper attempts to grasp or push the correct object by moving toward it and closing its jaws, but misses due to inaccurate positioning.

For real robot data, modifying actions directly is impractical due to current limitations of image editing and generation models. Therefore, we perturb the subtask text instruction paired with the pre-recorded trajectory segment (Fig. 2, bottom right) without direct robot control:

- (1) *Task-execution semantic mismatch* — an LLM (prompted with the original instruction and visible objects), or a rule-based preposition swap, generates a semantically altered instruction while preserving the start/end images.
- (2) *Revert action* — keep the instruction unchanged; replace the end image with the start one to show no progress.

Each execution example contains the task and subtask descriptions, plus pre-/post-action multi-view images.

TABLE I: Robot failure datasets sizes across splits.

Dataset	Training		Validation		Test	
	Exec	Plan	Exec	Plan	Exec	Plan
RoboFail [12]	-	-	-	-	153	30
RLBench-Fail	12358	5808	1000	500	1000	500
BridgeDataV2-Fail	7830	4880	1000	500	1000	500
UR5-Fail	400	200	30	30	140	140



Fig. 4: Failure mode distributions in real executions and our constructed data.

### C. Chain-of-Thought (CoT) Generation

CoT reasoning has shown promise in improving the interpretability and performance of VLMs [40]. Therefore, we further explore whether reasoning can help failure detection. We introduce an automatic method to generate step-by-step CoTs for training reasoning models. For each sample, we first collect the object category, spatial location, and robot state from the RLBench simulator or from ECoT [39] annotations, together with the corresponding failure reason. We then prompt a large reasoning-capable VLM (InternVL3-38B) [3] to generate step-by-step reasoning traces based on the initial text–image inputs and the aforementioned information. For planning samples, the model is instructed to sequentially verify each subtask and subsequently analyze the overall plan. For execution samples, the model is guided to describe the pre- and post-action images before assessing subtask completion. The reasoning trace contains 118 tokens on average. Fig. 3 illustrates training examples with chain-of-thoughts verifying plan correctness and subtask completion.

### D. Real-Robot, Policy-Driven Data Collection

We curate *UR5-Fail*, a real-robot dataset, collected using a UR5 arm with three cameras. We run the 3D-LOTUS++ policy [9] on 34 tasks, recording initial and final multi-view images for each subtask. Subtasks are manually labeled as success or failure to obtain execution failure data. For planning failures, we annotate ground-truth plans and generate failures using the method described in Sec. III-B. Unlike *RoboFail* [12], which is single-view and relies solely on teleoperation, *UR5-Fail* is three-view and features autonomous policy rollouts yielding more realistic failures.

### E. Dataset Statistics and Evaluation

The resulting datasets, *RLBench-Fail*, *BridgeDataV2-Fail*, and *UR5-Fail*, contain balanced success/failure examples

across both planning and execution, with fine-grained category labels and reasoning traces. Each dataset is split into training, validation, and test sets, with the validation and test sets featuring unseen tasks/environments to evaluate generalization. Dataset statistics are shown in Table I.

To measure the quality and diversity of our synthetic datasets, i.e., whether the generated failures reflect real policy execution, we run the 3D-LOTUS++ policy [9] on 92 RLBench tasks and manually annotate failure modes for 3 failure episodes per task. As shown in Fig. 4, our designed failure modes reflect real failures, and the overall distribution of our synthetic and real failures remains similar.

## IV. METHOD: THE GUARDIAN MODEL

### A. Problem Formulation

We formulate robot failure detection as a visual question answering problem. For planning verification, given a high-level task instruction  $T$ , a proposed plan  $P = (P_1, \dots, P_N)$ , and the initial visual context  $I_{\text{start}}$ , the model  $\text{VLM}_{\text{plan}}$  must not only decide whether the plan is correct but also categorize the type of failure when it occurs:

$$\text{VLM}_{\text{plan}}(I_{\text{start}}, T, P) \rightarrow (B_{\text{plan}}, C_{\text{plan}}), \quad (1)$$

where  $B_{\text{plan}} \in \{0, 1\}$  indicates whether the plan is valid, and  $C_{\text{plan}}$  specifies the failure category among the five planning failures constructed in Sec. III-B, shown in Fig. 4.

For execution verification, given the task goal  $T$ , a subtask description  $P_i$ , and the visual observations before and after execution,  $I_{\text{start}}$  and  $I_{\text{end}}$ , the model  $\text{VLM}_{\text{exec}}$  similarly outputs

$$\text{VLM}_{\text{exec}}(I_{\text{start}}, I_{\text{end}}, T, P_i) \rightarrow (B_{\text{exec}}, C_{\text{exec}}), \quad (2)$$

where  $B_{\text{exec}} \in \{0, 1\}$  indicates execution success, and  $C_{\text{exec}}$  denotes the execution failure category among the five execution failures constructed in Sec. III-B, shown in Fig. 4.

### B. Model Architecture

The *Guardian* model is built upon the state-of-the-art open-source VLM InternVL3-8B [3]. As illustrated in Fig. 5 (left), it consists of three key components: a text tokenizer that converts text prompts into discrete token embeddings, a visual encoder (InternViT-300M) that transforms individual images into visual embeddings, and a transformer-based LLM (Qwen2.5-7B) that processes the concatenated multimodal token sequence to predict the answer.

Rather than concatenating multiple images into a single grid-based image as in AHA [14], *Guardian* processes each image independently through the visual encoder. This design preserves fine-grained spatial details within each image and allows the model to explicitly reason about spatial and temporal changes for more accurate failure detection. Furthermore, unlike SuccessVQA [33] and AHA [14] that output direct classifications, *Guardian* leverages an explicit reasoning trace before concluding success or failure.

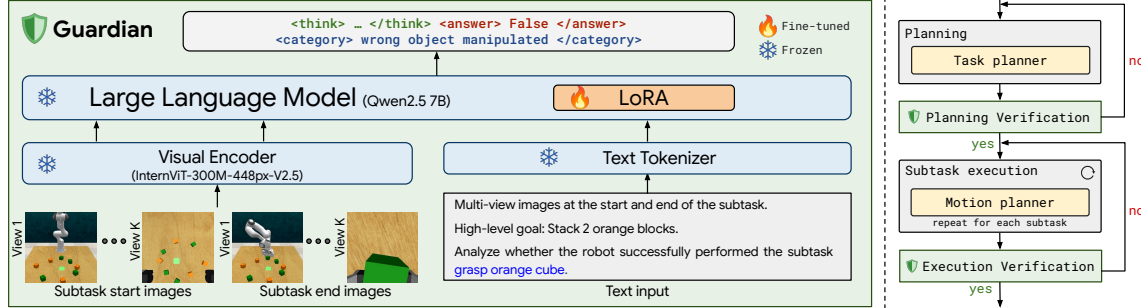


Fig. 5: Left: Overview of the *Guardian* model architecture. Right: Integration of *Guardian* model into a robot manipulation pipeline for planning and execution verification.

### C. Model Training

We fine-tune *Guardian* on robot failure datasets using parameter-efficient Low-Rank Adaptation (LoRA) [41], while freezing the visual encoder. Training minimizes cross-entropy loss for next-token prediction.

Although CoT has shown promise to improve performance, it brings additional computation overhead. Inspired by prior work [42], we explore three strategies for incorporating CoT into failure detection: (1) *Vanilla*: a baseline model trained and evaluated to directly predict final answers (*A*) without *CoT*; (2) *Thinking*: the model is trained and inferred with explicit reasoning, always generating *CoT* before *A*; (3) *Dropout*: in training, the model alternates between generating *CoT+A* and directly predicting *A*, while at test time, only *A* is produced.

### D. Integration into Robotic Manipulation Framework

*Guardian* can be seamlessly plugged into existing robotic manipulation pipelines as a verification layer without requiring any architectural modification. Without loss of generality, consider a modular robotic manipulation framework. As shown in Fig. 5 (right), *Guardian* can be inserted at each planning and subtask execution step to detect potential failures. Upon detection, it can trigger replanning or re-execute the corresponding motion policy to facilitate recovery.

## V. EXPERIMENTS

### A. Experimental Setup

**Evaluation datasets.** We evaluate models on our newly constructed benchmarks *RLBench-Fail*, *BridgeDataV2-Fail*, and *UR5-Fail*, as well as the existing benchmark *RoboFail* [12], which is a manually created real-world failure dataset using a UR5 arm with a single camera.

**Evaluation metric.** We report the mean binary detection accuracy for each dataset (success/failure) in Sec. V-B and discuss multi-class categorization in Sec. V-C.

**Implementation details.** We trained our models using LoRA (rank 16, effective batch size 16) with the AdamW optimizer (weight decay 0.05), bf16 precision, and a cosine learning rate schedule peaking at  $4 \times 10^{-5}$ . Training was conducted on the *RLBench-Fail* and *BridgeDataV2-Fail* sets (unless noted), completing in 5.5 hours on 4xH100 GPUs. During training, we randomly selected one or four views on *RLBench-Fail* data to mitigate overfitting to the multiple views. The best checkpoint is selected using the validation sets.

TABLE II: Comparison of SOTA failure detection models. Execution and Planning binary accuracies are reported. \* denotes numbers from the AHA paper. *Guardian* is fine-tuned from InternVL3-8B on our constructed datasets, boosting the performance of the base model by 23%.

(a) In-Domain datasets.

Model	RLBench-Fail		BDV2-Fail	
	Exec	Plan	Exec	Plan
<i>Large-scale generalist models</i>				
Qwen3-VL-235B-A22B	0.59	0.83	0.75	0.86
GPT4.1	0.63	<b>0.87</b>	0.72	0.86
<i>Specialized / small models</i>				
CLIP+MLP [43]	0.65	0.53	0.58	0.54
Sentinel [20]	0.57	-	0.57	-
Cosmos-Reason1-7B [33]	0.54	0.60	0.53	0.61
InternVL3-8B	0.59	0.70	0.66	0.71
Guardian-8B-Thinking	<b>0.83</b>	<b>0.87</b>	<b>0.85</b>	<b>0.91</b>

(b) Out-Of-Domain datasets.

Model	RoboFail [12]		UR5-Fail	
	Exec	Plan	Exec	Plan
<i>Large-scale generalist models</i>				
Qwen3-VL-235B-A22B	0.82	<b>0.70</b>	<b>0.79</b>	0.84
GPT4.1	0.82	0.67	<b>0.79</b>	0.88
<i>Specialized / small models</i>				
CLIP+MLP [43]	0.42	0.43	0.51	0.51
AHA-13B [14]	0.64*	-	-	-
Sentinel [20]	0.79	-	0.74	-
Cosmos-Reason1-7B [33]	0.67	<b>0.70</b>	0.58	0.63
InternVL3-8B	0.77	0.53	0.71	0.75
Guardian-8B-Thinking	<b>0.86</b>	<b>0.70</b>	0.77	<b>0.89</b>

### B. Comparison with state of the art

**Compared methods.** We compare our approach against SOTA general and specialized vision–language baselines. General baselines include small-scale (InternVL3-8B [3]), and large-scale models (Qwen3-VL-235B-A22B-Thinking [44], GPT4.1 [45]). Specialized baselines comprise Cosmos-Reason1-7B [33], AHA-13B [14], Sentinel [20], and an MLP baseline using CLIP text-image features [43]. We apply test-time CoT to the two large-scale models and Cosmos-Reason, as they are trained to produce reasoning traces and benefit from explicit reasoning at inference. Since AHA-13B is not publicly available, we report its binary accuracy on *RoboFail*

TABLE III: Impact of the Guardian fine-tuning data mix on the binary accuracy averaged over planning and execution.

Training Data			RLBench	BDV2	Robo	UR5
RLBench	BDV2	UR5	-Fail	-Fail	-Fail	-Fail
X	X	X	0.65	0.69	0.65	0.73
✓	✗	✗	0.80	0.72	0.69	0.74
✗	✓	✗	0.66	0.87	0.72	0.69
✓	✓	✗	<b>0.85</b>	<b>0.88</b>	<b>0.78</b>	0.83
✓	✓	✓	<b>0.85</b>	<b>0.88</b>	0.74	<b>0.85</b>

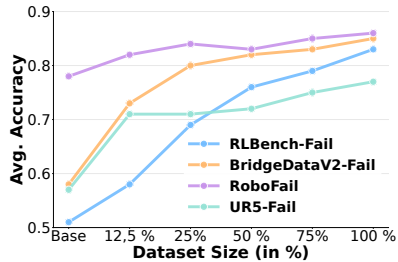


Fig. 6: Training data size impact on the Execution binary accuracy across benchmarks.

from the original paper [14]. Sentinel is limited to execution monitoring and is not evaluated for planning.

**Results.** Table II reports in-domain (ID) and out-of-domain (OOD) binary accuracies. Table IIa shows that our Guardian model, fine-tuned from InternVL3-8B on failure datasets, surpasses/matches the larger Qwen3VL and GPT4.1 on in-domain execution and planning sets. In Table IIb we evaluate models zero-shot on OOD datasets: Guardian attains 0.86/0.70 (Exec/Plan) binary accuracy on *RoboFail* and 0.77/0.89 on *UR5-Fail*, outperforming/matching larger general-purpose and specialized VLMs. Sentinel, applied atop Qwen3-VL, underperforms its base VLM, likely due to Sentinel’s rigid CoT prompt. Cosmos-Reason, trained on single-view binary failures, often overlooks fine-grained manipulator/object state changes. AHA, solely tuned to simulation failure data, does not generalize well to the real robot failures of *RoboFail*.

### C. Failure Data Ablations

In this section, we examine the composition and scale of our data, and discuss the multi-class categorization.

**Training data mixture.** Table III shows the impact of fine-tuning datasets. Row 1 is the baseline InternVL 3-8B without fine-tuning. Fine-tuning on simulated *RLBench-Fail* data (row 2) significantly improves the performance on the same dataset, but the gains do not transfer well to the other real-world datasets due to the domain gap. A similar trend is observed when training solely on *BridgeDataV2-Fail* in row 3. In contrast, combining both datasets during fine-tuning in the fourth row leads to significant gains in domain and improves generalization to the OOD benchmarks. This indicates the importance of generating diverse planning and execution data. Further fine-tuning with the small real-robot *UR5-Fail* dataset improves performance on *UR5-Fail* while maintaining comparable accuracy on the other datasets.

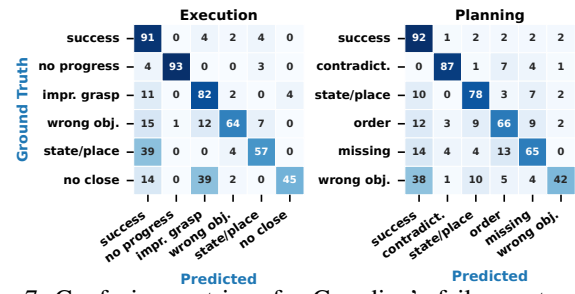


Fig. 7: Confusion matrices for Guardian’s failure categorization for plans and executions. Values are percentages; rows denote ground-truth classes and columns the predicted classes.

TABLE IV: Image representation impact on the Execution binary accuracy (number of views and image format). The AHA method [14] equals row 3 (4-view concatenation).

Views	Image Format	RLBench-Fail
		Execution
1	concat	0.61
	separated	0.63
4	concat (AHA [14])	0.72
	separated	<b>0.81</b>

**Training data size.** Fig. 6 presents the scaling behaviors of the training data size on the execution binary accuracies across *RLBench-Fail*, *BridgeDataV2-Fail*, *RoboFail*, and *UR5-Fail*. We observe a scaling behavior on in-domain and out-of-domain sets when fine-tuning on our procedurally generated data. This suggests that scaling the generated data size further could improve model performance.

**Multi-class Categorization.** Since our datasets contain fine-grained failure categorization, Guardian supports multi-class failure prediction. The confusion matrices in Fig. 7 show strong overall discrimination across categories. As shown in the Fig. 7(left), most execution categories are identified with high accuracy. The main weakness lies in the VLM’s visual grounding of subtle cues: *no gripper close* is confused with *imprecise grasping/pushing*, and *wrong object state or placement* is often mistaken for *success*. For planning shown in Fig. 7(right), *wrong object state or placement*, *wrong order*, *missing subtask*, and *wrong object manipulated* show higher confusion, particularly in long-horizon plans. Improving the model’s commonsense and temporal reasoning would further enhance its ability to capture these nuanced dependencies.

### D. Failure Detection Method Ablations

In this section, we compare visual representation choices and reasoning strategies for VLM-based failure detection.

**Multi-view images.** Table IV investigates the image representation choice on failure detection. We fine-tune and evaluate InternVL3-8B solely on *RLBench-Fail* execution data. We vary the number of viewpoints (one or four) and the multi-image format, either separated as in *Guardian*, or concatenated into a single image as in AHA [14]. For concatenated inputs, we represent the views as rows, and start/end images as columns. Using multi-view images consistently outperforms

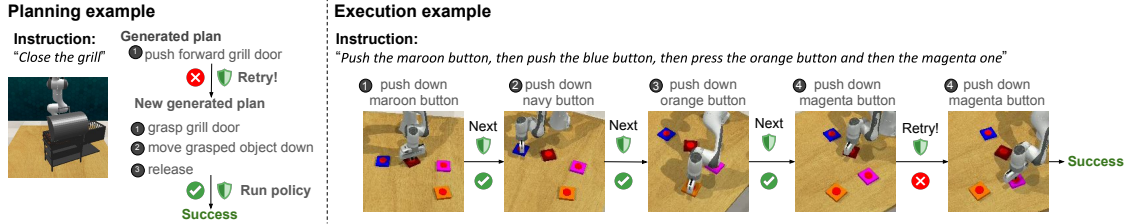


Fig. 8: Verification with *Guardian* during online task execution on RL Bench. Left: Successful correction of a generated plan. Right: Successful correction of a subtask execution.

TABLE V: Comparison of training and test-time strategies with and without CoT (Sec. IV-C). “A” denotes the final answer. We report the average binary accuracy and inference time [seconds/sample] on one H100.

Model	Training		Test		Avg. Accuracy	Inf.
	Output	Output	Exec	Plan		
Vanilla	A	A	0.81	0.78	0.68s	
Dropout	CoT, A	A	<b>0.83</b>	0.83	0.68s	
Thinking	CoT, A	CoT, A	<b>0.83</b>	<b>0.84</b>	4.3s	

TABLE VI: Success rate of the framework 3D-LOTUS++ with and without *Guardian* activated.

(a) RL Bench results across the four GemBench [9] levels.

Framework	Guardian	L1	L2	L3	L4
3D-LOTUS++	✗	0.57 $\pm$ 0.04	0.53 $\pm$ 0.03	0.23 $\pm$ 0.02	0.04 $\pm$ 0.01

(b) Real robot results in normal and perturbed setups.

Framework	Guardian	Put food		Arrange fruits		Stack cups	
		Norm	Pert	Norm	Pert	Norm	Pert
3D-LOTUS++	✗	0.60	0.00	<b>0.60</b>	0.20	0.80	0.00

their single-view counterpart. In the single-view setting, separating or concatenating two images (start and end) yields comparable performance, as the resolution loss from concatenation is minimal. However, in the four-view setting, separating the images significantly boosts the performance by 9 points over concatenation. Concatenating images not only shifts from natural image distributions but also compresses visual information in limited image resolution.

**Train-time and test-time CoT strategies.** We compare fine-tuning strategies and test-time output formats of *Guardian* described in Sec. IV-C. Table V shows the binary accuracy averaged across the four test sets. We find that training on reasoning traces can always improve the performance, which suggests that the CoT can improve internal representations of VLMs. The dropout strategy offers strong performance at low latency, while test-time CoT maximizes accuracy at the expense of inference speed (6 $\times$  slower).

### E. Downstream Robotic Tasks

**Simulation results.** To evaluate the practical utility of *Guardian*, we integrate it into 3D-LOTUS++ [9] and evaluate it across the 92 GemBench [9] task variations. GemBench assesses robot generalization capabilities across four levels: Level 1 (L1) with new locations, Level 2 (L2) with novel rigid objects, Level 3 (L3) with new articulated objects, and Level 4 (L4) with long-horizon tasks. For each task, we run 100 episodes (20 per seed across 5 seeds) and report the mean success rate ( $\pm$  standard deviation) with and without our verification module. The simulator reward is disabled to reflect better real-world conditions where such explicit signals are unavailable. If *Guardian* detects failures, we rerun up to 3 times the 3D-LOTUS++ planning or motion planning modules until *Guardian* outputs success. As shown in Table VIa, *Guardian* consistently improves success rates across the four levels, from 3% to 8%. Fig. 8 illustrates the online evaluation.

**Real robot results.** We deploy 3D-LOTUS++ [9] and *Guardian* into the same tabletop setup as used for collecting *UR5-Fail* (6-DoF UR5 robot, three RealSense D435 cameras). We fine-tune *Guardian* on *UR5-Fail* train set for this run, better calibrating the VLM to our setup (cf. Table III). We conduct evaluation on three unseen tasks: putting food into a box, arranging fruits on colored plates, and stacking colored cups. We assess the success rate both with and without *Guardian* over ten episodes (five under normal conditions and five with human-induced perturbations involving object translations or swaps). During perturbations, a human displaces objects to assess the policy’s recovery ability. As shown in Table VIb, *Guardian* improves success rates moderately under normal conditions (0–20%) and substantially under perturbations (20–80%). Fig. 9 shows the model’s predictions on a real-robot example for the putting food into a box task, where *Guardian* generates coherent reasoning traces and correctly identifies the failure. Additional examples are provided in the supplementary material.

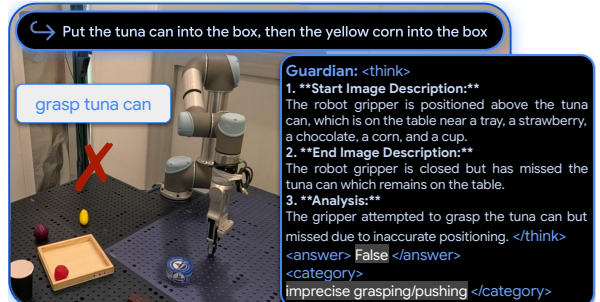


Fig. 9: Online evaluation of *Guardian* on a real-robot.

## VI. CONCLUSION

This work tackles the scarcity of data for training robotic failure detection models. We introduce an automated method that generates diverse planning and execution failures with detailed reasoning annotations in both simulation and real-world environments. This approach enables the construction of three new benchmarks: *RLBench-Fail*, *BridgeDataV2-Fail*, and *UR5-Fail*, which substantially expand the diversity and coverage of existing failure datasets. Using these datasets, we train *Guardian*, a vision-language model fine-tuned for failure detection, leveraging multi-view image inputs and step-by-step reasoning. *Guardian* achieves state-of-the-art performance on in-domain datasets and generalizes effectively to real-world settings without fine-tuning. With additional fine-tuning on real-robot data, its performance further improves, and we demonstrate how performance scales with more data. We further demonstrate *Guardian*'s plug-and-play utility by improving the task success rate of the 3D-LOTUS++ manipulation system in both simulation and real-robot experiments. Future work will investigate incorporating rich failure feedback directly into policy learning to enable more robust and autonomous recovery.

## VII. ACKNOWLEDGMENTS

This work was performed using HPC resources from GENCI-IDRIS (Grant 2025-AD011015795 and AD011015795R1). It was funded in part by the French government under management of Agence Nationale de la Recherche as part of the “France 2030” program, reference ANR-23-IACL-0008 (PR[AI]RIE-PSAI project), the ANR project VideoPredict ANR-21-FAI1-0002-01. Cordelia Schmid would like to acknowledge the support by the Körber European Science Prize.

## REFERENCES

- [1] Mistral AI. (2025) Mistral Small 3.1. Mistral Blog. [Online]. Available: <https://mistral.ai/news/mistral-small-3-1>
- [2] A. Grattafiori *et al.*, “The Llama 3 herd of models,” *arXiv preprint arXiv:2407.21783*, 2024.
- [3] J. Zhu *et al.*, “Internvl3: Exploring advanced training and test-time recipes for open-source multimodal models,” *arXiv preprint arXiv:2504.10479*, 2025.
- [4] R. Sinha *et al.*, “A system-level view on out-of-distribution data in robotics,” *arXiv preprint arXiv:2212.14020*, 2023.
- [5] K. Kawaharazuka, T. Matsushima, A. Gambardella, J. Guo, C. Paxton, and A. Zeng, “Real-world robot applications of foundation models: A review,” *AR*, 2024.
- [6] O. Kroemer, S. Niekum, and G. Konidaris, “A review of robot learning for manipulation: Challenges, representations, and algorithms,” *JMLR*, 2020.
- [7] W. Huang, P. Abbeel, D. Pathak, and I. Mordatch, “Language models as zero-shot planners: Extracting actionable knowledge for embodied agents,” in *ICML*, 2022.
- [8] L. Huang *et al.*, “A survey on hallucination in large language models: Principles, taxonomy, challenges, and open questions,” *ACM TOIS*, 2025.
- [9] R. Garcia, S. Chen, and C. Schmid, “Towards generalizable vision-language robotic manipulation: A benchmark and LLM-guided 3D policy,” in *ICRA*, 2025.
- [10] A. Goyal, J. Xu, Y. Guo, V. Blukis, Y.-W. Chao, and D. Fox, “RVT: Robotic view transformer for 3D object manipulation,” in *CoRL*, 2023.
- [11] K. Wu *et al.*, “Robomind: Benchmark on multi-embodiment intelligence normative data for robot manipulation,” in *RSS*, 2025.
- [12] Z. Liu, A. Bahety, and S. Song, “REFLECT: Summarizing robot experiences for failure explanation and correction,” in *CoRL*, 2023.
- [13] H. Chen, Y. Yao, R. Liu, C. Liu, and J. Ichnowski, “Automating robot failure recovery using vision-language models with optimized prompts,” in *CoRR*, 2024.
- [14] J. Duan *et al.*, “AHA: A vision-language-model for detecting and reasoning over failures in robotic manipulation,” in *ICLR*, 2025.
- [15] A. Khazatsky *et al.*, “DROID: A large-scale in-the-wild robot manipulation dataset,” in *RSS*, 2024.
- [16] E. Collaboration, “Open X-Embodiment: Robotic learning datasets and RT-X models,” in *ICRA*, 2024.
- [17] W. Pumacay, I. Singh, J. Duan, R. Krishna, J. Thomason, and D. Fox, “THE COLOSSEUM: A benchmark for evaluating generalization for robotic manipulation,” in *RSS*, 2024.
- [18] Q. Bu *et al.*, “Agibot world colosse: A large-scale manipulation platform for scalable and intelligent embodied systems,” in *IROS*, 2025.
- [19] W. Zhao, J. P. Queraltà, and T. Westerlund, “Sim-to-real transfer in deep reinforcement learning for robotics: a survey,” in *SSCI*, 2020.
- [20] C. Agia *et al.*, “Unpacking failure modes of generative policies: Runtime monitoring of consistency and progress,” in *CoRL*, 2024.
- [21] H. Etukuru *et al.*, “Robot utility models: General policies for zero-shot deployment in new environments,” in *ICRA*, 2025.
- [22] S. James, Z. Ma, D. R. Arrojo, and A. J. Davison, “RLBench: The robot learning benchmark & learning environment,” *IEEE RA-L*, 2020.
- [23] H. Walke *et al.*, “BridgeData V2: A dataset for robot learning at scale,” in *CoRL*, 2023.
- [24] G. De Giacomo, R. Reiter, and M. Soutchanski, “Execution monitoring of high-level robot programs,” in *KR*, 1998.
- [25] M. Gianni *et al.*, “A unified framework for planning and execution-monitoring of mobile robots,” in *AAAI Workshop*, 2011.
- [26] Y. J. Ma *et al.*, “Vision language models are in-context value learners,” in *ICLR*, 2025.
- [27] K. Shirai *et al.*, “Vision-language interpreter for robot task planning,” in *ICRA*, 2024.
- [28] M. Skreta, Z. Zhou, J. L. Yuan, K. Darvish, A. Aspuru-Guzik, and A. Garg, “RePLan: Robotic replanning with perception and language models,” *arXiv preprint arXiv:2401.04157*, 2024.
- [29] A. Mei, G.-N. Zhu, H. Zhang, and Z. Gan, “ReplanVLM: Replanning robotic tasks with visual language models,” *IEEE RA-L*, 2024.
- [30] Y. Du *et al.*, “Vision-Language models as success detectors,” in *CoLLAs*, 2023.
- [31] J.-B. Alayrac *et al.*, “Flamingo: a visual language model for few-shot learning,” in *NeurIPS*, 2022.
- [32] H. Liu, C. Li, Q. Wu, and Y. J. Lee, “Visual instruction tuning,” in *NeurIPS*, 2023.
- [33] NVIDIA *et al.*, “Cosmos-Reason1: From physical common sense to embodied reasoning,” in *CoRR*, 2025.
- [34] J. Wei *et al.*, “Chain-of-thought prompting elicits reasoning in large language models,” in *NeurIPS*, 2022.
- [35] Y. Ze, G. Zhang, K. Zhang, C. Hu, M. Wang, and H. Xu, “3D Diffusion Policy: Generalizable visuomotor policy learning via simple 3D representations,” in *RSS*, 2024.
- [36] K. Black *et al.*, “\$\\$ \backslash pi\\_0.5 \\$\$: a vision-language-action model with open-world generalization,” in *CoRL*, 2025.
- [37] J. Duan *et al.*, “Manipulate-Anything: Automating real-world robots using vision-language models,” in *CoRL*, 2024.
- [38] M. Shridhar, L. Manuelli, and D. Fox, “Perceiver-Actor: A multi-task transformer for robotic manipulation,” in *CoRL*, 2022.
- [39] M. Zawalski, W. Chen, K. Pertsch, O. Mees, C. Finn, and S. Levine, “Robotic control via embodied chain-of-thought reasoning,” in *CoRL*, 2024.
- [40] R. Zhang *et al.*, “Improve vision language model chain-of-thought reasoning,” in *ACL*, 2025.
- [41] E. J. Hu *et al.*, “LoRA: Low-rank adaptation of large language models,” in *ICLR*, 2022.
- [42] W. Chen *et al.*, “Training strategies for efficient embodied reasoning,” in *CoRL*, 2025.
- [43] A. Radford *et al.*, “Learning transferable visual models from natural language supervision,” in *ICML*, 2021.
- [44] Qwen Team. (2025) Qwen3-VL. Qwen Blog. [Online]. Available: <https://github.com/QwenLM/Qwen3-VL>
- [45] OpenAI. (2025) Introducing GPT-4.1 in the API. OpenAI Blog. [Online]. Available: <https://openai.com/index/gpt-4-1/>